

**FORWARD-BACKWARD FACING STEP PAIR: AERODYNAMIC FLOW, WALL PRESSURE AND ACOUSTIC CHARACTERISATION<sup>1</sup>**

Damien J.J. Leclercq

PSA Peugeot Citroën, Direction de la Recherche et de l'Innovation Automobile,  
F-78943 Vélizy-Villacoublay Cedex

Marc C. Jacob\*, Alain Louisot†

UMR CNRS 5509, Ecole Centrale de Lyon,  
F-69130 Ecully  
and

Corinne Talotte

Société Nationale des Chemins de Fer Français,  
F-7508 Paris**Abstract**

A two-dimensional subsonic air flow past a block mounted on a flat plate is investigated experimentally. The block is equivalent to a forward-backward facing step pair. It is shown that although the length-to-height ratio is high ( $L/h=10$ ), the flow separation at the backward facing step is strongly influenced by the oncoming perturbations of the forward facing one: the reattachment occurs 3.5 step heights downstream of the edge and the wall pressure field is influenced by eddies generated by the forward facing step separation. The latter also creates the strongest flow perturbations, resulting in a dominant contribution to sound radiation.

The experiment is carried out in the large anechoic room of the Ecole Centrale de Lyon. The  $h=0.05$  m high block is placed in an acoustically transparent channel and the corresponding Reynolds number based on the step height is  $1.7 \cdot 10^5$ . The boundary layer thickness of the incoming flow is about  $0.7 h$ . Measurements include a detailed Laser Doppler Anemometry analysis of the mean and fluctuating velocity field, in-depth measurements of the wall pressure fluctuations around the two steps, and streamwise source localisations obtained with a near field acoustic array.

**Nomenclature**

BWD : backward step  
 $d_{sensor}$  : diameter of pressure sensors  
 $\mathbf{e}_x, \mathbf{e}_y, \mathbf{e}_z$  : streamwise (x direction), cross-flow (y direction) and spanwise (z direction) unit vectors, respectively  
 $f$  : frequency  
 $f_{cutoff}$  : cut-off frequency of the wall pressure sensor

FWD : forward step  
 $h$  : steps height  
 $L$  : block length  
 $p$  : fluctuating pressure (acoustic or turbulent)  
 $q$  : dynamic pressure  $\frac{1}{2} \rho_0 U_0^2$   
 $R(x, \xi, \tau)$  : cross-correlation coefficient at position  $\mathbf{x}$ , for separation  $\xi$ , and delay  $\tau$ .  
 $S(\mathbf{x}, \xi, f)$  : cross-spectral density at position  $\mathbf{x}$ , for separation  $\xi$  and frequency  $f$ .  
 $\mathbf{U}(u, v, w)$  : velocity vector,  $u=U+u'$ ,  $U=\langle u \rangle$ ,  $v=V+v'$ ,  $w=W+w'$   
 $U_c$  : near wall convection speed  
 $U_0$  : free stream velocity  
 $U_p(\mathbf{x}, \xi, f)$  : phase speed  
 $\mathbf{x}(x, y, z)$  : position vector  
 $\gamma^2(\mathbf{x}, \xi, f)$  : coherence at position  $\mathbf{x}$ , for separation  $\xi$  and frequency  $f$ .  
 $\delta$  : incoming boundary layer thickness  
 $\phi(f)$  :  $= S(0, 0, f)$   
 $\xi(\xi, \eta, \zeta)$  : vector separating two points  
 $\rho_0$  : free stream air density

**1. Introduction**

Aeroacoustic sound generation is an important source of noise in high speed ground transportation. Geometrical singularities of the vehicle body are largely responsible for flow detachment, resulting in an increased aerodynamic sound radiation.

In the present paper the two dimensional flow past a rectangular block on a flat plate is examined. The configuration is both relevant from the industrial point of view and simple enough to be compared to well-known turbulent flows.

Past investigations (eg. Mohsen<sup>1</sup>, Moss & Baker<sup>2</sup>) are often concerned with short bodies (length to height ratio of 2 or less). They compare blocks to steps by

<sup>1</sup> Copyright © 2001 by the American Institute of Aeronautics and Astronautics, Inc. All rights reserved

\* also with Univ. Claude Bernard Lyon I, Villeurbanne, France

† now at Asea Brown Bowery-Solyvent-Ventec, 143, rue de la République, 69882 Mézioux.

means of flow reattachment properties (reattachment length, mean static pressure) but the radiated sound is not examined. For such short obstacles, the trailing edge is located in the separated flow of the leading edge: thus they do not behave as two separated singularities. As a result the flow downstream of the trailing edge is quite different from that due to an isolated backward facing step.

The present study is focused on a  $L/h=10$  block which has not been thoroughly investigated before to the authors' knowledge. The block trailing edge is thus located downstream of the reattachment of its leading edge. The flow is compared to some corresponding isolated step flows reported in the literature, from both the aerodynamic and acoustic standpoints.

Regarding the Wall Pressure Fluctuations (WPF), most studies carried out for strongly perturbed flow, since the early work on flat plate turbulent boundary layers back in the 50's, is about BWD and FWD steps, as well as short blocks (eg. Mohsen<sup>1</sup>, Farabee & Casarella<sup>3</sup>, Efimtsov<sup>4</sup>).

Mohsen<sup>1</sup> found that the dimensionless separation length varies little with flow velocity, and that the rms WPF levels are maximal at the point where the flow reattaches downstream of BWD steps, whereas it is maximal slightly before reattachment for FWD steps and blocks. He also stated that the measured levels are independent of step height. He described the evolution of the measured spectra with distance from the flow perturbation, and suggested that wall pressure fluctuations are proportional to the shear stress in the turbulent flow.

Farabee & Casarella<sup>3</sup> studied the effect of inflow turbulence, and reported detailed data for the BWD step. By scaling the wall pressure spectra on dynamic head and step height, these authors showed that the location of maximum spectral level moves from just upstream of reattachment for the low frequency components to downstream of reattachment for the higher frequencies. Moreover, the higher frequency components increase between the step and the reattachment, after which they tend to values that seem asymptotic.

Efimtsov *et al.*<sup>4</sup> report a parametric study of wall pressure fluctuations induced by BWD steps for Mach numbers ranging from 0.05 to 2.5, and step heights that are at most 1.5 times the boundary layer displacement thickness. Level are found to increase with step height. Auto power spectral densities are then modelled as a function of Mach number, dynamic pressure, step height, incoming boundary layer thickness, and flow speed. This function is to be added to the corresponding turbulent boundary layer spectrum.

In all three papers mentioned above, only the power spectra of the WPF are described as a function of distance from the step or the point of reattachment, with flow speed, incoming boundary layer thickness, and step height as parameters. The levels are much

higher (by up to 20 dB) than those measured beneath a turbulent boundary layer, over a considerable distance downstream of the step, estimated at 200 step heights by Efimtsov *et al.*<sup>4</sup>.

As for sound generation some results are available for backward facing steps under wall jets<sup>5</sup>: they show that the sound is mainly generated over a broad frequency range in the separated flow downstream of the step edge.

The scope of the present paper is to relate the flow field to the wall pressure field and to the radiated sound field. In section 2 the experiment is described. The mean and turbulent velocity fields are described in section 3 and the wall pressure field is discussed in detail in section 4. Section 5 shows the main acoustic sources of the flow.

## 2. Experimental set-up

### 2.1. Flow configuration

The experimental set-up (Figure 1) consists of a 50 m/s flow developing in the  $e_x$  direction on a hard, rigid aluminium, 0.5 m wide flat plate. A  $L=0.5$  m long,  $h=0.05$  m high, and 0.5 m large block is attached to the plate, thus constituting a series of two steps, a backward-facing (BWD) one which is located  $L=10h$  downstream of a forward facing (FWD) one. The step height to width ratio is thus equal to 0.1, which is the highest limit expressed by Moss & Baker<sup>2</sup> to obtain a two-dimensional flow in the symmetry plane.

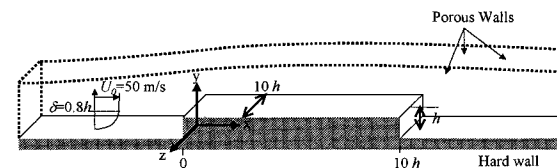


Figure 1 : Sketch of the experimental set-up

### 2.2. The facility

The experiment is carried out in the large anechoic facility at the Ecole Centrale de Lyon. The air is supplied into the anechoic room by an anechoic wind tunnel. It is guided into the room by a 3 m long square duct with a  $0.5 \times 0.5$  m<sup>2</sup> cross section. The flow is then accelerated by a contraction into a rectangular 3.5 m long channel which has a 0.5 m spanwise extent and a variable 0.25 to 0.35 m cross-stream extent. This channel has a massive aluminium floor, on which the block is mounted, and three acoustically transparent porous walls, developed by ECL. The acoustically transparent walls are made from a plastic gauze glued onto a 2 mm metal wire mesh, reinforced by a metal frame. This arrangement allows a correct source localisation through the walls. In order to prevent additional pressure gradients and to limit the flow trough the porous wall, the 'roof' (the

wall facing the floor) is shaped according to a mean flow streamline computed with an industrial k-ε industrial code. The channel thus constructed is 3.5 m long, with the FWD step 1.5 m from the upstream end. The channel exit is thus 1.5 m away from the BWD step, in order to remove jet type acoustic sources as far downstream as possible. This design provides a considerable improvement over a constant section channel at a reasonable design cost.

**2.3. Measurement techniques**

The flow velocity field in strongly perturbed regions was measured with Laser Doppler Anemometry (LDA). Its technical description can be found in previous papers<sup>5</sup>. The technique is checked against single hot wire anemometry in the non recirculating regions of the flow: the corresponding results are not reported here.

The Wall Pressure Fluctuations (WPF) measurement technique is described later in the paper. Auto- and Cross- Power spectral densities (PSD and CSD) were measured at several locations.

The radiated acoustic near field was measured in order to perform a source localisation. This was achieved with a linear near field array of 12 B&K ¼” microphones placed every 7 ± 0.05 cm parallel to the streamwise direction, 0.437 m away from the upstream wall (z=0, y= 0.487 ± 0.002 m). This array was placed over the block, its center facing the middle of the block (x=0.25 ± 0.003 m).

**3. Flow field**

Figure 2 presents the modulus of the mean velocity scaled on  $U_0$  near the FWD, and Figure 3 shows the corresponding velocity vectors. They clearly show that the flow accelerates to 15% above  $U_0$ , and separates into two bubbles on either side of the FWD step. The lines of flow inversion, i.e. where  $U$  changes near the horizontal walls or where  $V$  changes sign near the vertical wall, shows the mean locations of separation and reattachment.

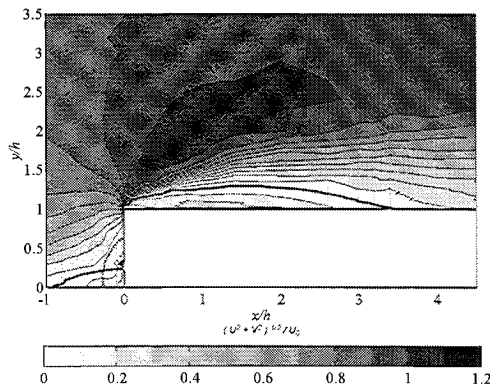


Figure 2 : Contours of the non dimensional modulus  $(U^2 + V^2)^{1/2} / U_0$  of the mean velocity near the FWD step ; the thick black lines are the lines where  $U$  (or  $V$  on the FWD step) changes sign.

The flow detaches 0.8  $h$  before the FWD step, reattaches on its vertical wall, at approximately 0.6  $h$ .

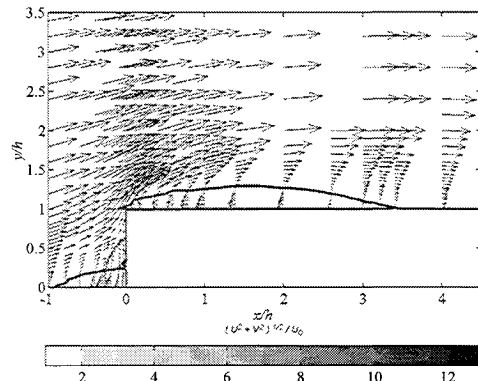


Figure 3: Vector plot of mean velocity near the FWD step

This flow separation does not generate a significant amount of turbulence as shown by the non dimensional streamwise fluctuations  $u'_{rms} / U_0$  on Figure 4. Cross-stream fluctuations have also been measured but are not represented here since they undergo the same variations as the streamwise ones with an amplitude which is about 50 % lower.

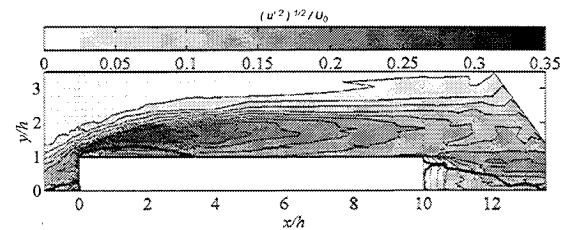


Figure 4: Streamwise velocity fluctuations  $u'_{rms} / U_0$

The sharp corner initiates another separation that extends 3.2  $h$  downstream of the FWD step. This value agrees with those found by Farabee & Casarella<sup>3</sup> which vary between 3 and 4  $h$  depending on flow configurations, but are higher than those found in open channel flows by Mohsen<sup>1</sup> which vary between 2 and 2.5  $h$ . Strong shear occurs at the edge, which results in a significant increase of turbulence as shown on Figure 4. Turbulence levels of up to 40% of  $U_0$  are reached in the shear layer that develops between the recirculating flow and the outer accelerated fluid. The highest levels are located in the first half of the separation region ( $x/h$  between 0 and 1.5).

As shown on Figure 5 and Figure 6, the flow separates again at the edge of the BWD step and reattaches about 3.5  $h$  downstream from it.

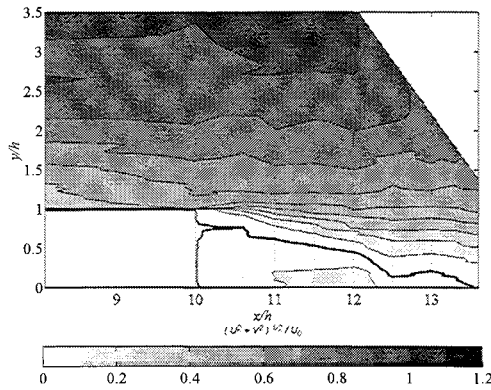


Figure 5 : Contours of the non dimensional modulus  $(U^2 + V^2)^{1/2} / U_0$  of the mean velocity near the BWD step. The thick black line is the line where  $U$  changes sign.

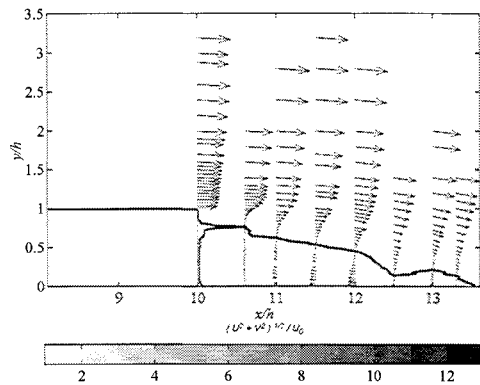


Figure 6: Vector plot of mean velocity near the BWD step

This value of the separation length is significantly lower than those observed for single BWD steps in classical channel flows<sup>3,6</sup> which vary between 6 and 8 step heights. The reason for this is twofold: the oncoming turbulence is significantly increased by the wake of the FWD step, resulting in an increase of cross-stream transfers; moreover streamwise pressure gradients do not build up in the channel because the acoustically non reflecting walls allow a pressure release. This effect of streamwise pressure gradients on the reattachment length has been reported by Kuehn<sup>7</sup> and the combination of a highly turbulent and a free turbulent flow resulting in such a short reattachment length has also been found by Jacob *et al*<sup>5</sup>. This reattachment length is also significantly lower than that found by Mohsen<sup>1</sup> downstream of a short block (11 to 12  $h$ ): this is not surprising since in Mohsen's study, the BWD step is located in the separated flow of the FWD step. This region downstream of the BWD step also generates high turbulence levels (up to 25% of  $U_0$ ) as shown on Figure 4 although turbulence levels remain quite smaller (about 50% less) than those generated by the FWD step. It can also be noticed that the highest

levels are reached between 2 and 3 step heights downstream of the edge, between 0.5 to 1 step height off the wall, just before reattachment occurs.

Similar conclusions are valid for the turbulent shear stress as shown on Figure 7: a negative peak value of  $-0.03 U_0^2$  downstream of the FWD step, and a local minimum value of about  $-0.015 U_0^2$  above the BWD step free shear layer are found. Note that both large zones of strong correlation have negative values, indicating either ejection of low speed fluid, or projection of high speed fluid towards the wall.

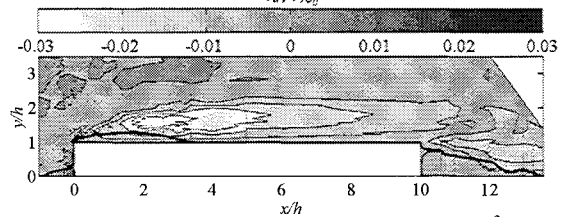


Figure 7 : Shear stress contours  $\langle u'v' \rangle / U_0^2$ .

#### 4. Wall pressure

##### 4.1. Mean pressure

The pressure coefficient is shown on Figure 8 : it increases to a maximum value of 0.43 at the bottom of the FWD step. The flow acceleration induces a strong pressure drop lower than  $-0.5$ , and the pressure stays negative down to the BWD step, where a second drop below  $-0.17$  occurs. Pressure becomes positive approximately  $2 h$  downstream of the reattachment point. Discrepancies with results reported by Farabee & Casarella<sup>3</sup> can be explained by the different experimental conditions, such as the acoustically transparent walls used in the present experiment which allow for a pressure release in the surrounding medium at rest. The static pressure distribution around the leading edge is thus characteristic of a FWD step flow, but differs from classical values on the BWD step (trailing edge), because the flow there is already highly perturbed by the upstream FWD step.

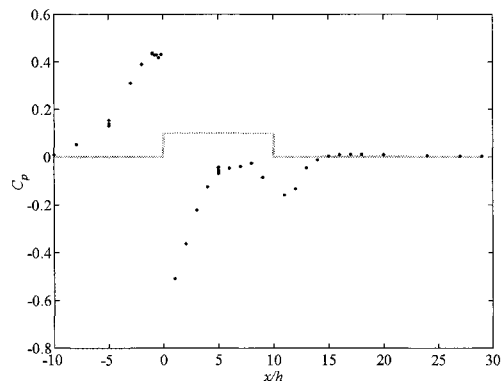


Figure 8 : Wall static pressure coefficients

**4.2. Wall Pressure Fluctuations (WPF)**

All results concerning the Wall Pressure Fluctuations are shown in the frequency domain. The present goal is to determine some properties of the forcing field applied on the wall, in order to ultimately predict the structural response of flexible panels subjected to a similar flow. Hence, after a description of the wall pressure measurement technique, the field is analysed in terms of Power Spectral Density (PSD). Then the spatial properties of the wall pressure field are examined by means of the Cross Spectral Density (CSD), from which convection speed and coherence information are derived.

**4.3. Measurement technique**

**Wall pressure transducers**

The wall pressure transducers used here were developed prior<sup>8</sup> to this work. They consist of a long capillary tube that is connected to an Sennheiser Ke4 Electret microphone through a pinhole drilled in its side. This design has been studied and used previously<sup>9,10</sup> and, although the accuracy for this type of transducer is a subject of controversy<sup>11,12,13</sup>, the measurements showed that the PSD obtained with these transducers were within 1 dB of the flush 1/8" microphone measurements in the frequency range of interest that is, for the present work, [35Hz 3.5kHz]. The wave propagation in the capillary tube induces a phase shift as well as an attenuation of the pressure signal transmitted to the microphone, and both can be corrected after transducer calibration. The calibration consists of a standard Frequency Response Function measurement between the wall pressure transducers and a reference B&K 4135 1/4" microphone. An example of such a correction function is displayed in Figure 9.

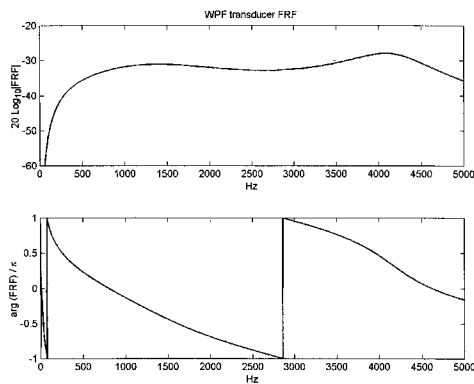


Figure 9 : Frequency Response Function measured for one of the wall pressure transducers. A weighting is used on the transducer channel only.

These transducers were mounted in the wall behind a 0.5 mm pinhole in order to minimise the effects of spatial averaging over the sensor surface<sup>14,15</sup>. These averaging effects are studied below.

**Transducers location**

The measurement points were chosen in the centre plane ( $z=0$ ): the transducers were located in pairs with a 1 cm separation, aligned either in the streamwise ( $\xi = 1$  cm) or the spanwise ( $\zeta = 1$  cm) direction. This allowed to measure the wall pressure PSD and CSD at different locations of the flow.

Downstream of the backward facing step reattachment, a rotating disc centred on a reference point 15  $h$  downstream of the step, 30 cm in diameter, equipped with 21 transducers, allowed an accurate scanning of the coherence field for a great number of positions relative to the reference point.

An array of transducers with various sensing diameters, from the flush mounted 1" B&K 4145 microphone, down to the 0.5 mm in-house WPF transducer, was positioned in the spanwise direction 10  $h$  downstream of the BWD step, to investigate the transducer spatial averaging effects in this region.

**4.4. Power Spectral Densities (PSD)**

Preliminary tests not reported here showed that all wall pressure spectra were free of spurious signals and that the WPF PSD were not significantly polluted by either acoustic waves or vibration above 40 Hz.

**Spatial averaging**

Figure 10 shows the wall pressure PSD obtained from transducers with various sensing diameters.

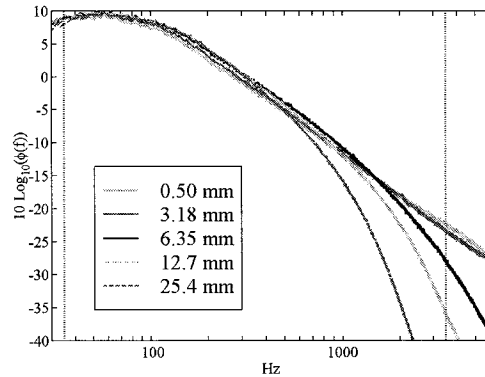


Figure 10 : PSD of WPF measured by transducers with various sensing diameters

The 1/8" microphone does not show any sign of attenuation due to spatial averaging, even up to 6 kHz, whereas the cut-off frequencies of the 1/4", 1/2" and 1" microphones, are approximately 1.8, 1, and 0.5 kHz respectively. Assuming the cut-off frequency to result from one frozen pattern convection velocity,  $f_{cutoff} = U_c / d_{sensor}$ , this convection velocity is found to be approximately 25% of the free-stream velocity. Note that these observations are valid in this region of the flow only, but measurements with the 0.5 mm diameter transducers can be assumed not to be affected by significant spatial averaging in the [35Hz - 3.5 kHz] range.

**Rms levels**

At about 1  $h$  upstream of the FWD step, the observed level is about 0.02 times the dynamic pressure  $q$  (Figure 11). Between the FWD and the BWD steps, the measurement resolution is not good enough to distinguish trends related to the separation bubble and reattachment. One can however observe that the rms level decreases from roughly 0.04  $q$  near the FWD step down to 0.025  $q$  towards the BWD step. Downstream of the BWD step, the maximal rms level (0.26  $q$ ) is reached about 2 to 3  $h$  downstream of the step, that is, just upstream of the reattachment point. These conclusions agree with those of Farabee and Casarella<sup>3</sup> upstream of a FWD step and downstream of a BWD step.

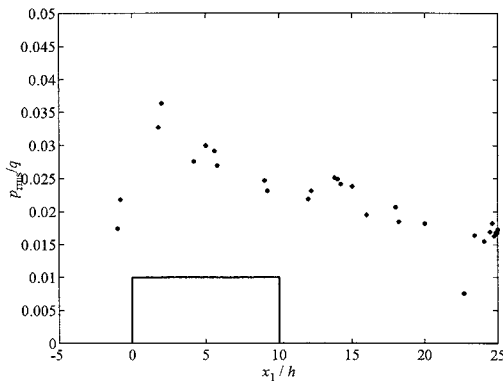


Figure 11 : WPF rms levels measured at various positions. [35 3500 Hz] bandwidth

As for the recirculation downstream of the FWD step, the maximum values are significantly lower than those observed by Farabee & Casarella<sup>3</sup>: they reach about 1/3 of their peak value. Reasons for such a discrepancy with their result can be a different incoming boundary layer thickness to step height ratio, the Reynolds number  $Re_h$  that is 5 to 8 times larger in our case, and also the poor spatial resolution in this area that does not allow a proper evaluation of the peak level.

**FWD step wall pressure PSD**

PSD measurements made 1  $h$  upstream of the FWD step show a decreasing function of frequency. Its particular location, close to the separation point, and the instability of this separation bubble do not allow a definite conclusion about this region.

As shown on Figure 12, the PSD measured downstream of the FWD facing step all reach a maximum at a frequency that slowly decreases from  $\omega h/U_0 \approx 0.9$  (145 Hz), at a 2  $h$  distance from the step, down to 0.79 (125 Hz) at 9  $h$ . The peak in the PSD thus exists beyond the reattachment point, at a dimensionless frequency  $\omega h/U_0$  close to 1. As mentioned for the overall levels, the peak levels also decrease very slowly with increasing distance from the step, even beyond the reattachment line.

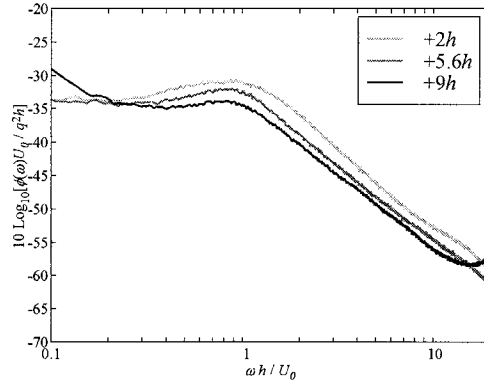


Figure 12 : WPF PSD at different stations downstream of the FWD step. The high frequency positive slope at 9  $h$  from the step is identified as a calibration problem.

The spectra decrease as a  $-2.5$  to  $-2$  power law of the frequency. The FWD step generates a perturbation in the WPF that survives well beyond the reattachment point, and the PSD evolves gently over the explored area.

**BWD step wall pressure PSD**

The picture is quite different downstream of the BWD step. Figure 13 below shows wall pressure PSD measured between 2 and 15  $h$  away from the step.

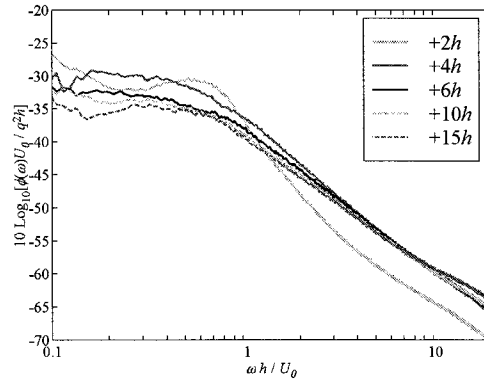


Figure 13 : PSD of the WPF measured downstream of the BWD step.

Two distinct shapes of spectra appear, depending on the position relative to the reattachment point. Under the separation bubble, the PSD shows a local maximum at 80 Hz ( $\omega h/U_0 \approx 0.5$ ), and a fairly steep negative slope in the higher frequencies (approximately  $f^{-3}$  in the medium range,  $f^{-2}$  above). Beyond reattachment, this peak disappears, and the PSD decreases over the observed frequency range. As measurements are taken further downstream of the reattachment, the low frequency content decreases, whereas the level increases in the high frequency range, resulting in flatter spectra, more similar to those of a flat plate turbulent boundary layer.

When scaled on step variables, measurements downstream of the BWD step are in good agreement with the PSD published by Farabee & Casarella<sup>3</sup>, in terms of absolute levels and trends. It is interesting to note, however, that these authors measure a peak beyond the reattachment point. The present data do not allow such an observation in the frequency range of interest, possibly because the FWD step induces perturbations that modify the BWD step flow properties, mainly by lowering the characteristic frequency of the separated flow wall pressure fluctuations. In order to characterise the influence of the FWD step on the BWD step, the coherence between transducers located at various positions upstream of the BWD step (-1 to -8  $h$  from the edge) and one located 2  $h$  downstream of the edge under the recirculation bubble is measured (Figure 14). The coherence is indeed maximal around  $\omega h/U_0 \approx 0.5$  (~80 Hz) for which the maximal PSD level is found beneath the BWD step recirculation (Figure 13). Similar measurements upstream and downstream of the FWD step not shown here, prove that no coherent information is convected past the obstacle, since the step is higher than the incoming boundary layer thickness.

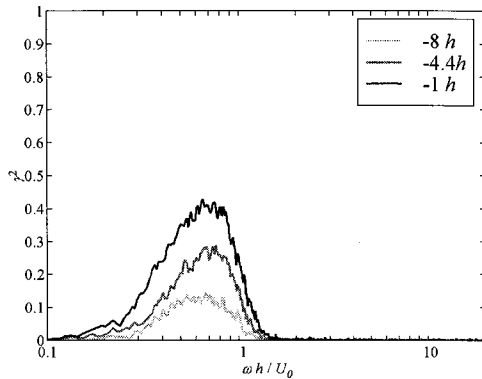


Figure 14 : Wall pressure coherence measured between various transducers upstream of the BWD step, and one transducer 2  $h$  downstream of the step. The distances in the legend are measured from the step.

#### 4.5. Cross spectral densities (CSD)

Cross spectral densities are physically interpreted as the product of PSD, a decay term (the coherence  $\gamma^2$ ), and a phase term that represents, in this case, convection:

$$S(\mathbf{x}, \xi, f) = \phi(\mathbf{x}, f) \gamma(\mathbf{x}, \xi, f) e^{-i2\pi f \xi / U_p(\mathbf{x}, \xi, f)}$$

The PSD was described above and the present paragraph is dedicated to the coherence and the phase speed as a function of frequency and spatial separation. The shape and properties of these functions are important for the computation of the dynamic response of a panel subjected to a similar

excitation, using a modal decomposition approach. These functions are evaluated at different positions in the flow for streamwise and spanwise transducer pairs with a 1 cm separation distance. The phase velocity is only measured along the main flow direction.

#### FWD step wall pressure CSD

Around the FWD step upstream separation point, the WPF coherence (not displayed here) peaks at  $\gamma^2=0.55$  for  $\omega h/U_0 \approx 0.25$ , and decreases towards 0 for increasing frequencies when  $\omega h/U_0$  is larger than 3. This weak coherence can be explained by the nature of the flow in this region, where there is very little convection between the two transducers. In these conditions, phase velocity is difficult to estimate, and is approximately 40 % of the free stream velocity. The separation bubble downstream of the FWD step allows a much more accurate description of the coherence evolution. Measurements 1.9  $h$ , 5.7  $h$ , and 9.1  $h$  away from the step show a peak in the coherence at a frequency of  $\omega h/U_0 \approx 1$  (Figure 15). Away from the step, the coherence peak level increases and becomes broader, but its frequency remains the same. This frequency also corresponds to that of the maximum level observed on the PSD beneath the recirculation bubble.

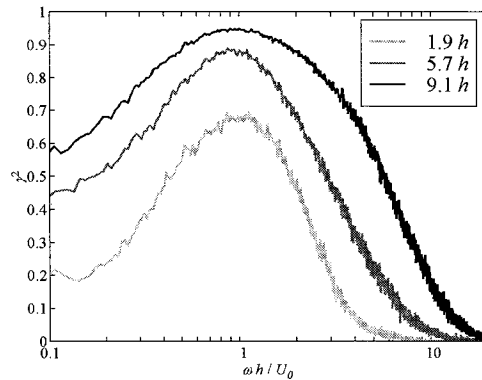


Figure 15 : Coherence measured for 1 cm streamwise separation at various positions downstream of the FWD step.

In the low frequency range the phase velocity is measurable, and increases away from the separation bubble, where the flow is less perturbed by this separation (Figure 16). Outside the bubble, the velocity peaks at the same frequency as the coherence. With increasing frequency, the phase velocity decreases down to a high frequency limit. This limit increases slightly away from the step.

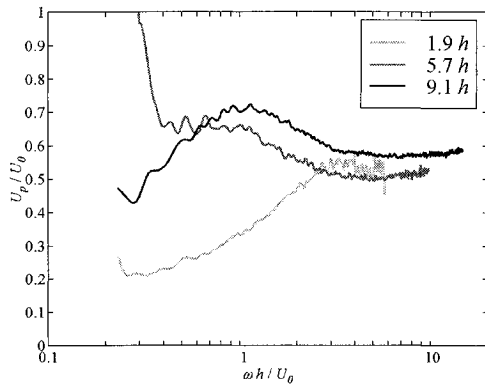


Figure 16 : Phase velocity estimated from three transducer pairs (1 cm streamwise separation) downstream of the FWD step.

On Figure 17, spanwise coherence downstream of the FWD is characterised in terms of a frequency dependent isotropy factor, which is the ratio of spanwise to streamwise coherence. On this figure, spanwise, streamwise as well as the isotropy factor are plotted against frequency. The isotropy factor shows that the coherence field, otherwise strongly anisotropic, tends to isotropy at the peak frequency (the ratio approaches unity).

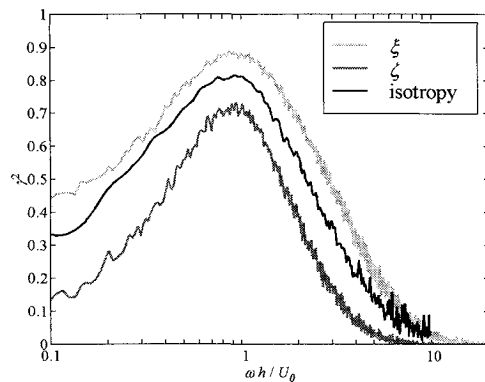


Figure 17 : Wall pressure coherence 5.8 h downstream of the FWD step, 1 cm separation: Streamwise coherence, spanwise coherence, and ratio of the latter and the former.

The FWD step flow thus produces energy in the WPF signal in a relatively narrow frequency range centred on  $\omega h/U_0 = 1$ . In the same frequency range, the wall pressure field is strongly coherent and its coherence becomes almost isotropic.

**BWD step wall pressure CSD**

Downstream from the BWD step, similar features can be observed: Figure 18 shows a narrow coherence peak centred on the frequency of the PSD maximum. This peak broadens away from the step, giving evidence of the fact that a wider variety of turbulent length scales are generated. It is also interesting to

note the slight frequency decrease between the recirculating flow, where the narrow peak is centred around 0.6, and the attached one for which a maximum is observed at a dimensionless frequency 0.4, 4 h after the step. The low frequency increase of the coherence shown on Figure 18 can be explained by the fact that the measurement zone is located near the averaged reattachment point, and thus can be subjected to the low frequency oscillations of the impinging shear layer.

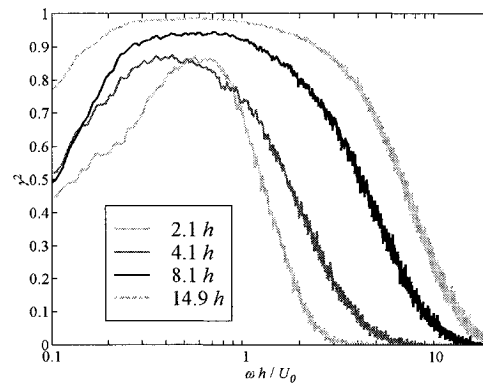


Figure 18 : 1 cm streamwise coherence measured at various locations downstream of the BWD step.

Figure 19 shows the streamwise and spanwise coherence measured 2 h downstream of the BWD step for a 1 cm separation. The similarity between the two functions, which both have the same peak at a frequency  $\omega h/U_0 \sim 0.6$ , is striking.

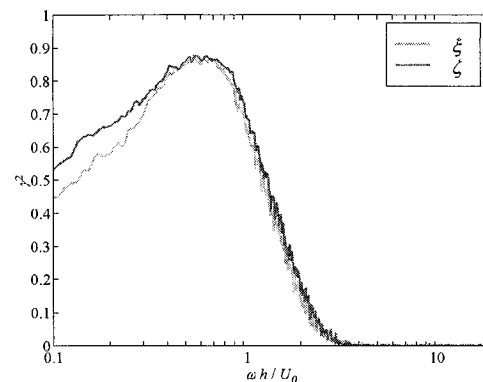


Figure 19 : Streamwise and spanwise coherence measured for 1 cm separations, 2 h downstream of the BWD step.

In this case, the wall pressure field induced by the separated flow shows a strong and isotropic coherence around the frequencies of highest energy ( $\omega h/U_0 < 1$ ). The coherence drops sharply with increasing frequency. Although no transducer triplet was available in the FWD step separated flow region, one could assume a similar behaviour in that region.

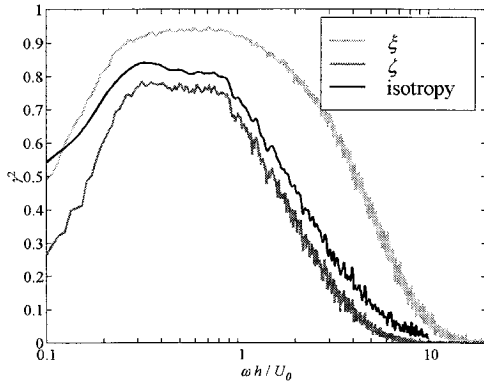


Figure 20 : Streamwise, spanwise coherence, and isotropy factor measured for 1 cm separations, 8 h downstream of the BWD step. of the BWD step.

Well beyond reattachment, 8 h away from the BWD step, the coherence becomes anisotropic again in the less energetic part of the spectra ( $\omega h/U_0 > 1$ ) as shown on Figure 20. This behaviour is similar to what can be observed on Figure 17, except that the high, isotropic, coherence region extends to lower frequencies ( $\omega h/U_0 \approx 0.3$ ) in the present case, because of the large turbulent scales generated in the recirculation shear layer that gradually evolves into a reattached turbulent boundary layer.

The phase velocity displays the same trends as those observed for the FWD step, i.e. an increase as the reattached flow relaxes from its perturbation.

**A closer investigation of the coherence field**

The pressure coherence field was carefully examined 15h downstream of the BWD step. Both isotropy and levels were studied for various frequencies. The rotating disk described in the “Transducers location” section of § 4.3, is designed to give a good spatial resolution of the W.P.F. coherence field in all directions.

Figure 21 and Figure 22 show the results obtained for two typical frequencies. In order to obtain contour plots some smoothing was required. The reprocessed data was compared to the raw data to make sure that it remained faithful to the measurements. The black dots on the figures represent the actual values of the separation ( $\xi, \zeta$ ) for which measurements were made. In this region, the flow is reattached and returning to a turbulent boundary layer: thus coherence is again strongly anisotropic because of strong convection effects.

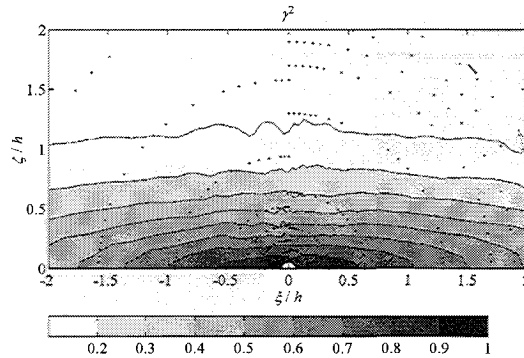


Figure 21 : Measured coherence as a function of the streamwise and spanwise separation, 15 h downstream of the BWD step.  $\omega h/U_0=1$

At all frequencies the coherence contours have the shape of an ellipse, in agreement with previous experimental<sup>16</sup> and numerical<sup>17</sup> work on turbulent boundary layers. This, of course, does not support the modelling of the coherence for off-axis directions as the product of a streamwise and a spanwise coherence function.

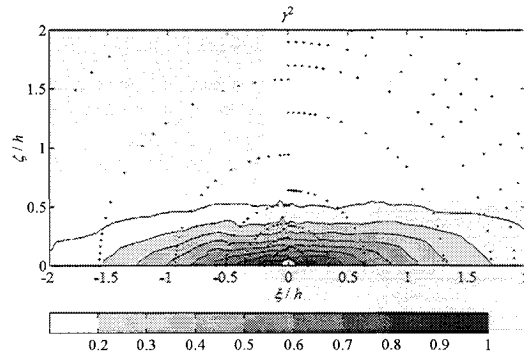


Figure 22 : Id. Figure 21,  $\omega h/U_0=2$

**4.6. Velocity / wall pressure coherence**

In order to link the turbulent velocity field to the wall pressure fluctuations, the coherence was measured between a single hot wire probe located above the centre of the rotating disc, and the wall pressure transducer at the centre of the disc. The coherence was measured for various cross stream positions ( $\gamma$ ) of the hot wire.

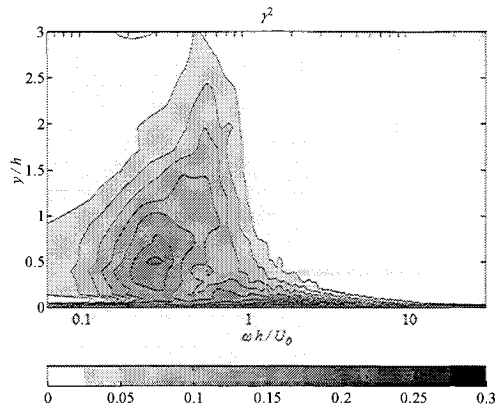


Figure 23 : Coherence between the single hot wire anemometer located above a wall pressure transducer, 15 h downstream of the BWD step.

In the vicinity of the wall, coherence levels are important in the whole frequency range. Coherence levels higher than  $\gamma^2=0.15$  are measured when the hot wire is located within 1 h from the wall at frequencies ranging from  $\omega h/U_0=0.2$  to 0.4. This shows that the wall pressure fluctuations measured in this region are a trace of flow patterns located one step height away from the wall.

### 5. Radiated sound

The acoustic near field is measured with the microphone array described in section 2.3.

The localisation technique compares the cross-spectrum matrix obtained from the experiment to the matrix constructed from a streamwise distribution of uncorrelated monopoles: an iterative algorithm searches for the best fitting streamwise intensity distribution of monopoles for each frequency from 200 Hz to 5 kHz. All acoustic signals are processed by a Hewlett Packard multichannel data analyser, which is controlled from a PC by an HP software.

Figure 24 shows a typical result obtained at  $U_0=50\text{m/s}$ . Acoustic levels from different streamwise locations ( $x$ ) felt by the array are plotted against the frequency. The shades of grey show the relative level of the dominant radiating sources. It can be seen on Figure 24 that the FWD step is the dominant source in this flow. It is located between 1 and 2 step heights downstream of the edge, that is in the middle of the recirculation bubble and radiates mostly for frequencies up to 2.5 kHz. Another significant source is located between 2 and 3 step heights downstream of the BWD step, just upstream of the reattachment point. The plot indicates that this source radiates at lower frequencies than the main source (up to 1 kHz at 50 m/s) and is not as powerful. The localisation gives a precise picture of the source distribution at frequencies higher than 500 Hz, but lacks resolution in the frequency range examined in the WPF study: thus the two investigations give a different view of the flow unsteadiness and the question whether the

low frequency unsteadiness radiates sound or not, remains open. Both sources are located in the regions of maximal turbulence described in section 3. This seems to indicate that the sound sources are due to the turbulence created in the separated flows. However, the possible amplification by the nearby edges can not be excluded from these results since the edges are located within a wavelength, which is about the resolution of the localisation technique.

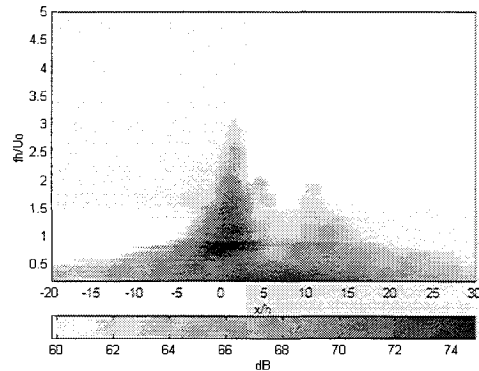


Figure 24 : Source localisation at 50 m/s

### 6. Conclusions

The flow past a backward facing (BWD) step located 10h downstream of a forward facing (FWD) one has been studied in terms of flow velocity statistics, wall pressure mean values and fluctuations, and radiated acoustic field.

It has been found that the flow past the FWD step reattaches 3.2 h downstream of the step edge, that is 6.8 h upstream of the BWD step. The flow around the FWD step has the typical features reported in the literature. This is not the case for the BWD step flow which is strongly perturbed by the wake of the FWD step. The oncoming FWD step perturbations result in a significantly reduced reattachment length ( $\sim 3h$ ) of the BWD step flow which is shorter than the values measured in classical channel flows. It also modifies considerably the Wall Pressure Fluctuation (WPF) field: the WPF under the BWD step recirculation bubble shows evidence of the remainders of the coherent structures generated by the FWD step. Moreover, the WPF investigations show that its coherence is almost isotropic under the recirculation bubbles whereas spanwise coherence is less pronounced than streamwise coherence in other, attached, flow regions. Furthermore, maximal WPF levels are located in the vicinity of the reattachment. Another significant difference between the two steps is that the FWD step generates the strongest perturbation levels, as shown by all measurements of unsteady fields: the velocity fluctuations and the wall pressure fluctuations both reach their highest levels in the FWD step separated flow region. Sound source localisations show that the sound originates from the two regions of maximal turbulence and that the FWD source is accordingly dominant. In terms of frequency

ranges, the WPF highlights the low frequency unsteadiness of the flow separations which appear to be centred around preferred frequencies. The source localisation is more focused in the higher frequency range and identifies rather broad band sources localised in the free shear layers evolving from flow separations at the steps.

### Acknowledgements

This work was supported by the French Ministère de l'Education Nationale, de la Recherche et de la Technologie.

### References

- <sup>1</sup> Mohsen, A. M. , 1967, "Experimental investigation of the wall pressure fluctuations in subsonic separated flows", *Boeing Commercial airplane division report No D6-17094*.
- <sup>2</sup> Moss, W.D. & Baker, S. 1980 "Re-circulating flows associated with two-dimensional steps", *Aero. Quart. Aug1980* pp.151-172.
- <sup>3</sup> Farabee, T. M. & Casarella, M. J., 1984, "Effects of Surface irregularity on turbulent boundary layer wall pressure fluctuations", *Journal of Vibration, Acoustics, Stress and reliability in Design*, **160**, pp.343-350.
- <sup>4</sup> Efimtsov, B.M., Kozlov, N.M., Kravchenko, S.V. & Andersson A.O., 2000, "Wall-pressure fluctuation spectra at small backward-facing steps" *AIAA Paper n° 2000-2053 6<sup>th</sup> AIAA/CEAS Aeroacoustics Conference and Exhibit 12-14 June 2000, Lahaina, HI, USA.*
- <sup>5</sup> Jacob, M. C., Gradoz, V. , Louisot, A., Juve, D. & Guerrand, S., 1998, "Sound produced by a backward facing step under a wall jet", *AIAA paper n° 98-230*.
- <sup>6</sup> Eaton J. K. & Johnston, J. P. 1981, "A review on subsonic turbulent flow reattachment", *AIAA J.*, **19(9)**, pp. 1093-1099.
- <sup>7</sup> Kuehn, D. M., 1980, "Effects of adverse pressure gradient on the incompressible reattaching flow over a rearward facing step", *AIAA J.*, **38(3)**, pp. 41-51.
- <sup>8</sup> Leclercq, D. J. J., 1999, "Modélisation de la réponse vibro-acoustique d'une structure couplée à une cavité en présence d'un écoulement turbulent". *Ph D. Thesis, Département Génie Mécanique, Université de Technologie de Compiègne*.
- <sup>9</sup> Mahan, J.R. & Karchmer, A. , 1991, "Aeroacoustics of Flight Vehicles: Theory and Practice Volume 1: Noise Sources", NASA TR 903052 edited by H.H. Hubbard, pp. 504-507.
- <sup>10</sup> Gabard, S., 1994, "Contribution à l'étude de l'influence d'une liaison pneumatique sur la transmission et la mesure des fluctuations de pression", Ph D. Thesis, *Centre d'Etudes Aérodynamiques et Thermiques, Université de Poitiers*.
- <sup>11</sup> Bull, M. K. & Thomas, A. S. W. , 1976, "High frequency wall pressure fluctuations in turbulent boundary layers", *Physics of Fluids* **19**, pp. 597-599
- <sup>12</sup> Farabee, T. M. & Casarella, M. J., 1991, "Spectral features of wall-pressure fluctuations beneath turbulent boundary layers", *Physics of Fluids A* **3**, pp. 2410-2420.
- <sup>13</sup> Bull, M. K., 1996, "Wall-pressure fluctuations beneath turbulent boundary layers: some reflections on forty years of research", *Journal of Sound and Vibration* **190**, pp.299-315.
- <sup>14</sup> Corcos, G. M. , 1963, "Resolution of pressure in turbulence", *Journal of the Acoustical Society of America* **35**, pp. 192-199.
- <sup>15</sup> Schewe, G. , 1983, "On the structure and resolution of wall pressure fluctuations associated with turbulent boundary-layer flow", *Journal of Fluid Mechanics* **134**, pp. 311-328.
- <sup>16</sup> Smol'yakov, A. V. & Tkachenko, V. M., 1991, "Model of a field of pseudosonic turbulent wall pressures and experimental data", Translated by J.S. Wood, *Sov. Phys. Acoust.* **37(6)**, pp. 627-631.
- <sup>17</sup> Singer, B. A., 1996, "Turbulent wall pressure fluctuations: new model for off-axis cross spectral density", *NASA Contract NAS1-20059*.